Thermochimica Acta 511 (2010) 51–58

Contents lists available at ScienceDirect

Thermochimica Acta

journal homepage: www.elsevier.com/locate/tca

Nonisothermal reaction, thermal stability and dynamic mechanical properties of epoxy system with novel nonlinear multifunctional polyamine hardener

Jintao Wan, Bo-Geng Li*, Hong Fan**, Zhi-Yang Bu, Cun-Jin Xu

State Key Laboratory of Chemical Engineering, Department of Chemical and Biochemical Engineering, Zhejiang University, Hangzhou 310027, China

ARTICLE INFO

Article history:
Received 30 May 2010
Received in revised form 19 July 2010
Accepted 22 July 2010
Available online 30 July 2010

Keywords:
Epoxy resin
Nonlinear polyamine
Nonisothermal reaction kinetics
Málek method
Dynamic mechanical properties
Vyazovkin method

ABSTRACT

N,N,N′,N′-tetra(3-aminopropyl)-1,6-diaminohexane (TADH), a nonlinear multifunctional polyamine, was prepared and employed as a novel hardener for diglycidyl ether of bisphenol A (DGEBA). Nonisothermal reactions of DGEBA/TADH were systematically investigated with differential scanning calorimetry (DSC). According to the Málek method, the two-parameter Šesták–Berggren model was selected to simulate the reaction rate with a good match achieved, and a correlation of effective activation energies E_α with fractional conversion α was determined with the mode-free isoconversional Vyazovkin method. As α rose, E_α reduced quickly from ~65 to 57 kJ/mol up to $\alpha \approx 15\%$, then decreased slowly to ~50 kJ/mol till $\alpha \approx 75\%$, and finally dropped to ~30 kJ/mol at full conversion. In addition, analysis of thermal stability of the cured DGEBA/TADH with thermogravimetric analysis (TGA) revealed that it possessed quite good thermal stability and increased residual char content at 600 °C in nitrogen. Furthermore, dynamic mechanical analysis (DMA) of the DGEBA/TADH network showed its relaxations were characterized by localized motions of hydroxyl ether segments (β relaxation) and cooperative motions of whole network chains (glass relaxation) at different temperature regions.

1. Introduction

Epoxy resins have long been used in protective coatings, adhesives, sealant, fiber-reinforced composites, molding compounds, and electronic encapsulation and insulating materials worldwide, due primarily to their high rigidity, excellent chemical resistance, good electric insulation properties, superior adhesion, easy processing and shaping, and wide formulation diversity. To achieve desired end-use properties, linear or branched epoxy monomers or oligomers must be transformed into a crosslinked network polymer via copolymerization with various hardeners, or via homopolymerization in the presence of suitable catalysts. In practical applications, the most commonly used epoxy resins are diglycidyl ether of bisphenol A (DGEBA) of various molecular weights, whereas amine-based hardeners hold the largest share in epoxy hardener markets accordingly [1–4].

In general, bulk properties of epoxy resins are largely determined by their chemistry and compositions, and strongly affected by curing and processing conditions as well [5]. For a given epoxy formulation, thus, linking curing conditions to properties is always a good policy of optimizing ultimate performances of epoxy resins. In this sense, reaction kinetics of epoxy resins plays an extremely important role in determining their curing and processing conditions, and has appealed numerous research efforts over the past decades [6,7]. Apart from vastly studied reaction kinetics of linear epoxy systems, noticeably considerable attention has been paid to reaction kinetics of nonlinear multifunctional epoxy systems. For instance, nonlinear tetrafunctional and trifunctional epoxy resins have received much attention due to their superior performances over their linear analogues arising from their nonlinear molecular architecture and extraordinary high epoxy functionality densities [8–18]. Alternatively, in principle nonlinear multifunctional amine hardeners may, in essence, function as their nonlinear epoxy counterparts in an epoxy system; however, relevant kinetic information on these epoxy-amine reaction systems is still rather sparse in open literature to date [6,19–22], due to limitation of suitable hardeners available.

In addition, thermal stability of epoxy resins is very critical in determining their application temperature ranges and in predicting service time [23], and hardeners affect greatly thermal stability of cured epoxy resins [24]. More importantly, dynamic mechanical properties of epoxy materials are a necessary consideration for their bear-loading applications [25], and a solid knowledge of dynamic mechanical properties of epoxy resins can help us to illuminate characteristics of specific epoxy networks and their thermal-mechanical properties at a more fundamental level [26,27]. As a result, the dynamic mechanical properties of epoxy networks with linear amine hardeners have long received substantial research interest [28–34]. As far as we know, however, dynamic

* Corresponding author. Tel.: +86 571 87952623; fax: +86 571 87951612.
** Corresponding author. +86 571 87957371; fax: +86 571 87951612.
E-mail addresses: bgli@zju.edu.cn (B.-G. Li), hfan@zju.edu.cn (H. Fan).

0040-6031/$ – see front matter © 2010 Elsevier B.V. All rights reserved.
doi:10.1016/j.tca.2010.07.024

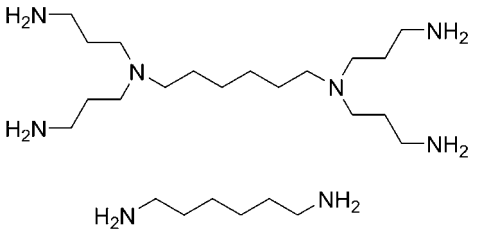

Scheme 1. Molecular structures of TADH and hexanediamine.

mechanical properties of epoxy networks with nonlinear amine hardeners are still rarely addressed in open literature to date [35], due largely to lack of appropriate hardeners.

Therefore, it is highly desirable to exploit new nonlinear amine hardeners of good thermal stability, and to acquire a better understanding of reaction kinetics and dynamic mechanical properties of epoxy resins cured with them from fundamental and practical application perspectives, which stimulates us to conduct the current work. This paper dealt with a unique epoxy system consisting of stoichiometric DGEBA and N,N,N′,N′-tetra(3-aminopropyl)-1,6-diaminohexane (TADH), a novel nonlinear polyamine hardener. The nonisothermal reaction kinetics of DGEBA/TADH was systematically studied using a dynamic DSC technique; in addition, thermal stability and dynamic mechanical properties of its cured product were evaluated with TGA and DMA, respectively.

2. Experimental

2.1. Materials

Hexanediamine (Scheme 1) and acrylonitrile were purchased from Shanghai Reagent Co., Ltd., China, and purified by distillation under reduced pressure prior to use. Diglycidyl ether of bisphenol A (DGEBA) was obtained from Heli Resin Co. Ltd., China with EEW of 196 g/equiv., and dehydrated in vacuum after use. N,N,N′,N′-tetra(3-aminopropyl)-1,6-diaminohexane (TADH) was synthesized via the bimolecular Michael addition of hydrogen atoms of the primary amine functionalities of 1,6-diaminohexane onto activated double bonds of acrylonitrile under favorable conditions, followed by heterogeneously catalyzed reduction of the intermediate polynitriles to the corresponding primary polyamine (TADH) [36,37]. The molecular structure of TADH is illustrated in Scheme 1, and its FTIR, ^{1}H-NMR, and ESI-MS spectrum data are given below. These data agree well with the predictions from its theoretical molecular structure, indicating full achievement of TADH. To be clearer, the ^{1}H-NMR spectrum of TADH is presented in Fig. 1 where the assignments of chemical shifts for different kinds of protons are highlighted.

TADH: FTIR (ν_{max}, cm^{-1}) 3345, 3290 (NH_2), 2933, 2856, 2803, 1574 (NH_2), 1469, 1382, 1312, 1087, 821. ^{1}H-NMR (400 MHz, $CDCl_3$, δ ppm) 1.20, m, 4H, $NCH_2CH_2C\underline{\mathbf{H}}_2C\underline{\mathbf{H}}_2CH_2CH_2N$; 1.25, s(broad), 8H, $N\underline{\mathbf{H}}_2$; 1.35, m, 4H, $NCH_2C\underline{\mathbf{H}}_2CH_2CH_2C\underline{\mathbf{H}}_2CH_2N$; 1.51, m, 8H, $NH_2CH_2C\underline{\mathbf{H}}_2$; 2.30, t, 4H, $NC\underline{\mathbf{H}}_2CH_2CH_2CH_2CH_2C\underline{\mathbf{H}}_2N$; 2.37, t, 8H, $NH_2CH_2CH_2C\underline{\mathbf{H}}_2$; 2.65, t, 8H, $NH_2C\underline{\mathbf{H}}_2$. ESI-MS: $[M+1]^+$ = 345.3.

2.2. DSC characterization

A Perkin Elemer differential scanning calorimeter (DSC-7) was previously calibrated with indium standard and then used to trace nonisothermal reactions of DGEBA/TADH. The dynamic DSC runs were performed at heating rates of 5, 10, 15 and 20 °C/min under N_2 purge (20 ml/min), temperature ranging from 25 to 250 °C. Stoichiometric DGEBA and TADH (NH:EP = 1:1) were mixed quickly at room temperature with vigorous agitation, until a transparent solution was obtained. Then, the fresh reaction mixture of about 10 mg was sealed in an aluminum pan, and subjected to a dynamic temperature scan with an empty pan as the reference. Furthermore details about how to acquire and process thermal data could be accessed elsewhere [6].

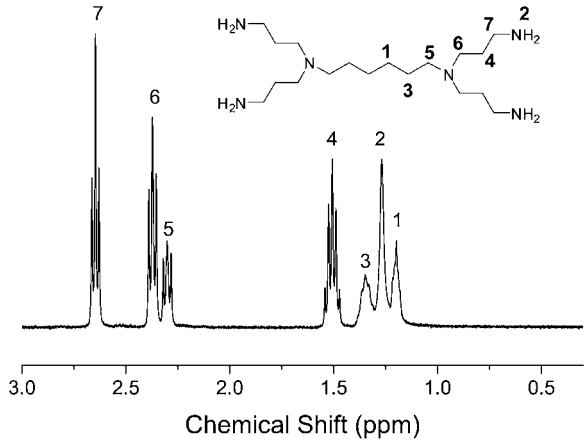

Fig. 1. ^{1}H-NMR spectrum of TADH.

2.3. TGA measurement

Thermal stability of cured DGEBA/TADH was evaluated with a thermogravimetric analyzer (Pyris 1 TGA) at a heating rate of 10 °C/min from 40 to 600 °C under a nitrogen flow (40 ml/min). Moreover, linear hexanediamine was used as the controlled hardener, and cured DGEBA/hexanediamine was examined with TGA under the same condition.

2.4. DMA testing

Dynamic mechanical properties of the fully cured stoichiometric DGEBA/TADH casting (70 °C/1.5 h + 150 °C/2.5 h) as a function of temperature were studied using a TA dynamic mechanical analyzer (DMA Q800). Dimension of the specimen was 35 mm × 10 mm × 2 mm; heating rate was 3 °C/min; temperature ranged from −100 °C to well above the glass temperature; specimen clamp was the single-cantilever one; loading frequency was 1 Hz; oscillation amplitude was 15 μm.

3. Results and discussion

3.1. Kinetic fundamentals

DSC is a powerful and most convenient tool for investigating exothermic reactions of epoxy resins due to its great accuracy and easy sample preparation. Reaction heat measured with DSC is assumed to be directly proportional to reacted epoxy groups, so that conversion of epoxy groups and reaction rate can be written by Eqs. (1) and (2), respectively [38–41]:

$$\alpha = \frac{\int_0^t Q dt}{\int_0^{t_f} Q dt} \quad (1)$$

$$\frac{d\alpha}{dt} = k(T) f(\alpha) \quad (2)$$

In the above equations, α is the extent of cure or the conversion, Q is the heat flow measured with DSC, t is the reaction time, t_f is the time to reaction completion, $f(\alpha)$ is the model-dependent function of α, T is the reaction temperature, and $k(T)$ is the reaction rate constant which follows the Arrhenius law:

$$k(T) = A \exp\left(-\frac{E_a}{RT}\right) \tag{3}$$

where A is the pre-exponential factor or the frequency factor, E_a is the activation energy, and R is the universal gas constant.

On the basis of Eqs. (2) and (3), generally two main kinetic methods frequently cited have been derived to study the reaction kinetics epoxy resins: the model-fitting method and the model-free isoconversional method [42]. For the former, one needs to select a kinetic model previously, and then fit experimental thermal data with a selected model to estimate unknown model parameters. Ultimately, an explicit rate equation can be established to predicate advancement of epoxy reactions. In practices, various empirical kinetic models as summarized by Málek [43–45] have been most frequently used to describe kinetics of nonisothermal processes including epoxy reactions. In this case, for a specific nonisothermal process how to select an appropriate reaction model and how to calculate a set of kinetic parameters become very crucial in model-fitting kinetic studies, due to strong mutual compensation among kinetic triple, A, E_a and $f(\alpha)$, which sometimes leads to great uncertainty in kinetic parameters, especially in E_a [44,46,47]. Málek [43,45] have proposed a method to guide judicious selection of reaction models and rational calculation of involved model parameters for a thermally stimulated physical or chemical process under linear temperature programs. Up to date, a considerable number of scholars have successfully applied the Málek method to nonisothermal reactions of different epoxy systems including epoxy-amine [6,45,48–51], epoxy-acid anhydride [52–57], epoxy-phenolic [58] and epoxy-imidazole [59].

According to the Málek method, apparent activation energy E_a for a nonisothermal process must be known previously, and then the two special functions $y(\alpha)$ and $z(\alpha)$, Eqs. (4) and (5), can be defined as the diagnostic signatures for determination of reaction models and for calculation of model parameters.

$$y(\alpha) = \left(\frac{d\alpha}{dt}\right) \exp(x) \tag{4}$$

$$z(\alpha) = \pi(x)\left(\frac{d\alpha}{dt}\right)\frac{T}{\beta} \tag{5}$$

In Eqs. (4) and (5), x is the reduced activation energy E_a/RT, β is the heating rate, and $\pi(x)$ is the function of temperature integral [60] which can be numerically approximated with sufficient accuracy using a fourth-order rational equation derived by Senum and Yang [61]:

$$\pi(x) = \frac{x^3 + 18x^2 + 88x + 96}{x^4 + 20x^3 + 120x^2 + 240x + 120} \tag{6}$$

Then, examine whether couture and peak conversions (α_M, α_p^∞) of the normalized $y(\alpha)$ and $z(\alpha)$ functions and conversion α_p corresponding to maximum experimental rates satisfy a set of specific conditions proposed by Málek [43,45], and then one can probably confirm an appropriate kinetic model and further obtain a method to calculate model parameters. In this context, the Málek method has been used to investigate the model-fitting kinetics of the nonisothermal DGEBA/TADH reactions.

On the other hand, the model-free kinetic method builds on the isoconversional principle that states kinetic rate at a give conversion is only a function of temperature [42,62,63]; see Eq. (7):

$$\left[\frac{d\ \ln\left(d\alpha/dt\right)}{dT^{-1}}\right]_\alpha = -\frac{E_\alpha}{R} \tag{7}$$

where α represents the specific conversion, and E_α is the effective activation energy for α. In essence, Eq. (7) is an isoconversional differential method equivalent to famous Friedman method [63]. This method has the greatest advantage of processing the nonisothermal and isothermal data with the same computing method; however, it always produces unstable E_α values, because of quite noisy rates obtained from numerical differentiation of experimental α vs. T curves [64]. To overcome this obstacle, later model-free isoconversional integral methods have been proposed, and they can be grouped into two general categories: the linear method and the nonlinear one [65]. For the former, E_α at any α can be graphically evaluated through linear transformation of multiple nonisothermal data under certain approximations [66,67]. In thermal analyses of nonisothermal processes, the most frequently used is FWO method [68,69]:

$$\ln \beta_i = \text{Const.} - \frac{1.052E_a}{RT_{\alpha,i}} \tag{8}$$

where i is the thermal experimental ordinal.

As regards the nonlinear method, it takes the advantage of free of any linear approximations as in the FWO method, and the advanced isoconversional method developed by Vyazovkin (Vyazovkin method) is an excellent paradigm [42,70,71]. The Vyazovkin method is based on accurate integration of Eq. (3), thus effectively eliminating systematic errors generated when applying the FWO method [71,72]. The general analytic expressions for the Vyazovkin method can be written by:

$$\Phi(E_\alpha) = \sum_{i=1}^{n}\sum_{j\neq i}^{n}\frac{J\left[E_\alpha, T_i(t_\alpha)\right]}{J\left[E_\alpha, T_j(t_\alpha)\right]} = \min \tag{9}$$

$$J[E_\alpha, T_i(t_\alpha)] \equiv \int_{t_{\alpha-\Delta\alpha}}^{t_\alpha} \exp\left[\frac{-E_\alpha}{RT_i(t)}\right] dt \tag{10}$$

where subscripts, i and j, denote the different experimental ordinals with varied heating programs, $\Delta\alpha$ is the increment of conversion which is usually set as 0.02 sufficient to eliminate accumulative errors in E_α calculation, t is the reaction time which is a function temperature in a nonisothermal process, J is the temperature integral [60] which can be numerically evaluated with certain algorithms [70,71], and other parameters have the same meanings as in Eq. (7). According to this method, a set of experiments should be performed under varied temperature programs to generate sufficient conversion–temperature (α–$T(t)$) data, and then E_α can be determined at any particular α by minimizing Eq. (9). Repeat this minimization procedure for each α of interest, ultimately giving rise to an E_α–α correlation. Noticeably, nowadays an increasing number of workers have successfully applied this method to untangling reaction mechanisms of epoxy resins, with much new and unusual findings revealed [6,22,62,64,73–87], increasing the impact of this method. Therefore, here we have also used the Vyazovkin method to analyze the mechanisms of the nonisothermal DGEBA/TAHD reaction.

3.2. Nonisothermal reaction of DGEBA/TADH

Fig. 2 presents the DSC thermographs of heat flow as a function of temperature for the nonisothermal reaction of DGEBA/TADH at the heating rates of 5, 10, 15 and 20 °C/min. Obviously, each of the DSC runs shows a single exothermic peak of fairly good

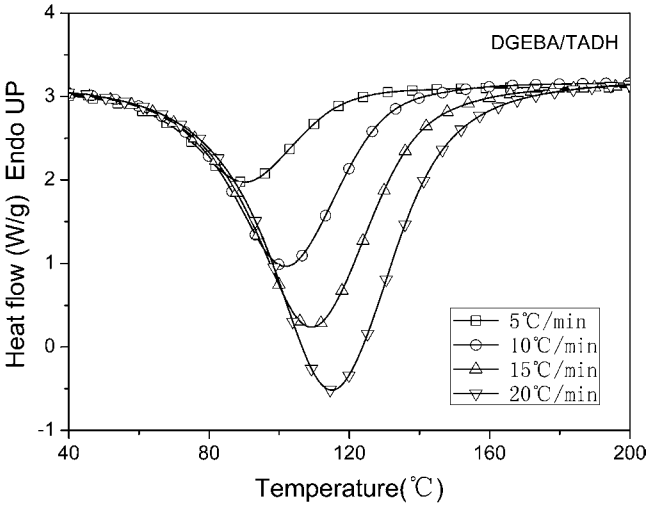

Fig. 2. Nonisothermal thermographs of DGEBA/TADH reactions at heating rates of 5, 10, 15 and 20 °C/min.

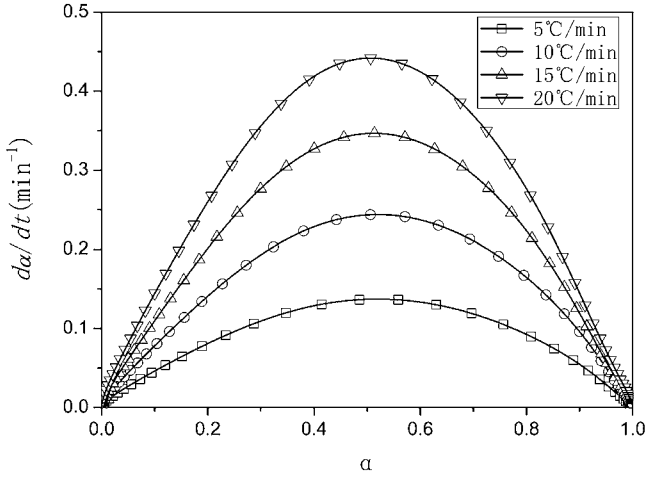

Fig. 3. Reaction rate $d\alpha/dt$ as a function of conversion α at heating rates of 5, 10, 15 and 20 °C/min.

symmetry without any shoulders, which likely suggests the nonisothermal reactions can be considered as a single kinetic process from a statistical viewpoint. Increasing the heating rates results in the exothermic peak shifting to an increasingly high and broad temperature range with the systematically elevated onset reaction temperature and the peak temperature, T_{onset} and T_p, as shown in Table 1. In addition, the overall reaction heat ΔH_R for the different heating rates is estimated by integrating the heat flow curve with respect to the linear baselines, and their values are listed in Table 1. Clearly, the heating rate little influences ΔH_R within the experiment errors, which suggests that the nonisothermal reaction of DGEBA/TADH can achieve an identical absolute reaction extent. Noticeably, ΔH_R of DGEBA/TADH (117.8–121.2 kJ/mol epoxide) falls within the typical values (98–122 kJ/mol epoxide) collected from a large number of epoxy-amine reactions [6,38,88–94]. This agreement indicates that TADH can effectively cure epoxy resins with an acceptable ultimate reaction extent under ambient reaction conditions.

Transform the thermal data in Fig. 2 with Eq. (1), followed by differentiation with respect to t, and then the reaction rate $d\alpha/dt$ as a function of α results, as seen in Fig. 3. Obviously, increasing the heating rates leads to systematically increased $d\alpha/dt$; that is, $d\alpha/dt$ is a positive function of the heating rate at same α. Nevertheless, maximum $d\alpha/dt$ appears at an essentially constant conversion of ≈0.50 independent of the heating rates, which likely implies that the fundamental reaction mechanisms remain unchanged.

3.3. Apparent reaction activation energy

Knowing apparent reaction activation energy E_a is a prerequisite of model selection according to the Málek method, and in this study the most frequently cited Kissinger method [95] have been applied for this purpose. According to this method, when a set of nonisothermal reactions carry out under different linear heating programs, the Kissinger equation holds [95]:

$$\ln\left(\frac{\beta}{T_p^2}\right) = \text{Const.} - \frac{E_a}{RT_p} \tag{11}$$

where β is the heating rate, T_p is the peak exothermic temperature for β, and E_a is the apparent activation. Then, according to Eq. (11) the resulting slop of linear plot of $\ln(\beta/T_p^2)$ against $-1/T_p$ can be used to calculate E_a. Here the Kissinger plot of $\ln(\beta/T_p^2)$ vs. $-1/T_p$ for the nonisothermal reaction of DGEBA/TADH is shown in Fig. 4 from which an excellent linear correlation is found (R = 0.99996). As a result, E_α is 58.82 kJ/mol which is consistent with typical results (50–70 kJ/mol) for a number of epoxy-amine polymerizations [82,92,96–98].

Table 1
Characteristic parameters for nonisothermal reactions of DGEBA/TADH at different heating rates of 5, 10, 15 and 20 °C/min.

β (°C/min)	T_{onset} (°C)	T_p (°C)	ΔH_R (J/g)	ΔH_R (kJ/mol)
5	61.2	89.8	492.8	117.8
10	70.3	101.9	503.0	120.3
15	76.9	109.5	506.8	121.2
20	80.9	114.7	500.8	119.7

3.4. Kinetic modeling

Substitute E_α, $d\alpha/dt$, T and β into Eqs. (3)–(5), and we can obtain normalized $y(\alpha)$ and $z(\alpha)$ using the Software Origin 7.5, as shown in Figs. 5 and 6. Apparently, $y(\alpha)$ reaches its maximum at essentially constant conversion $\alpha_M \approx 0.20$, while the maximum value of $z(\alpha)$ occurs at $\alpha_p^\infty \approx 0.52$; meanwhile, the experimental rate peak conversions appear at $\alpha_p \approx 0.51$, as shown in Fig. 3. Table 2 summaries the values of α_M, α_p^∞ and α_p, from which we can find that they

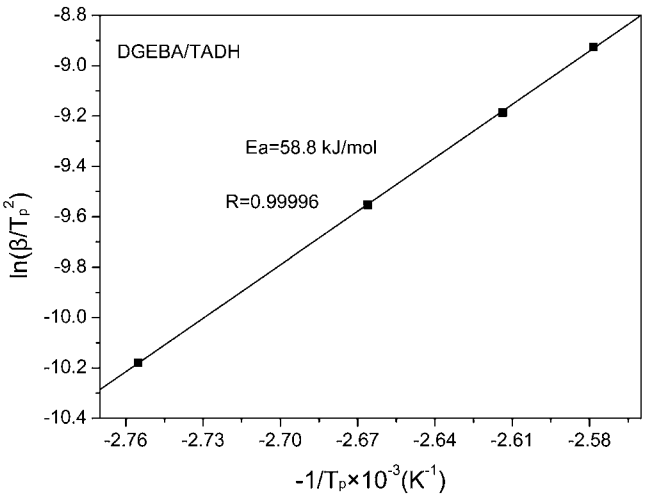

Fig. 4. Kissinger plot of $\ln(\beta/T_p^2)$ vs. $-T_p^{-1}$.

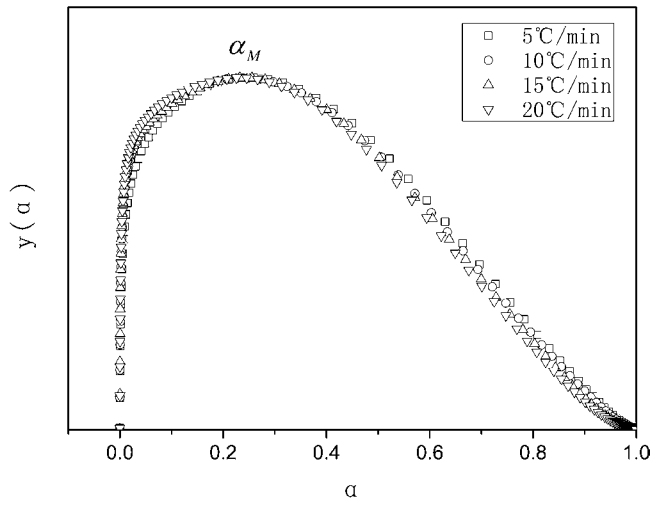

Fig. 5. Plots of normalized $y(\alpha)$ against α at heating rates of 5, 10, 15 and 20 °C/min.

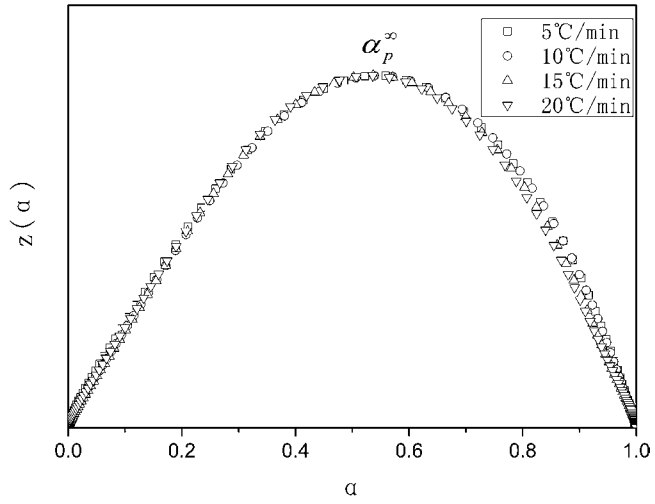

Fig. 6. Normalized $z(\alpha)$ as a function α at heating rates of 5, 10, 15 and 20 °C/min.

simultaneously fulfill $\alpha_p^\infty \neq 0.623$ and $\alpha_M < \alpha_p < \alpha_p^\infty$ for the same heating rate. According to the criteria proposed by Málek [43,45], therefore, we can confirm that the autocatalytic Šesták–Berggren model (Eq. (12)) [99] should be used to describe the nonisothermal reaction rate of DGEBA/TADH:

$$\frac{d\alpha}{dt} = A \exp\left(-\frac{E_a}{RT}\right)\alpha^m(1-\alpha)^n \quad (12)$$

In Eq. (12), the ratio of reaction order m to n, $p = m/n$, as pointed out by Málek [43,45], can be replaced by:

$$p = \frac{\alpha_M}{(1-\alpha_M)} \quad (13)$$

where α_M is the conversion for peak value of $y(\alpha)$ function (Eq. (4)).

Table 2
Characteristic peak conversions α_p, α_M and α_p^∞.

Heating rate β (°C/min)	α_p	α_M	α_p^∞
5	0.504	0.248	0.542
10	0.513	0.239	0.545
15	0.521	0.244	0.537
20	0.522	0.235	0.535
Mean	0.515	0.242	0.540

Table 3
Estimated kinetic parameters, m, n and $\ln A$, for Šesták–Berggren model.

Heating rate β (°C/min)	m	n	$\ln A$ (min^{-1})	R
5	0.444	1.347	18.779	0.99982
10	0.434	1.382	18.752	0.99977
15	0.485	1.499	18.837	0.9997
20	0.476	1.547	18.842	0.99969
Mean	0.460	1.440	18.802	–

Then, logarithmic transformation and rearrangement of Eqs. (12) and (13) yield:

$$\ln\left[\left(\frac{d\alpha}{dt}\right)\exp(x)\right] = \ln A + n \ln\left[\alpha^p(1-\alpha)\right] \quad (14)$$

With Eq. (14), we can determine the reaction order n and pre-exponential factor A from the slope and the intercept of the linear plot of $\ln[(d\alpha/dt)\exp(x)]$ *vs.* $\ln[\alpha^p(1-\alpha)]$ for $\alpha \in [0.1, 0.9]$, respectively. Note here that due to the peak tails (dense sampling points but slow reaction rate) of nonisothermal DSC runs which will lead to high errors [45,51], thus the extreme conversion ranges should be excluded in calculation of the kinetics parameters. The obtained m, n and $\ln A$ for the Šesták–Berggren model are summarized in Table 3. Evidently, the heating rates affect slightly these model parameters, without the variation exceeding 10% of their mean values. Finally, substitution of their mean values into the Šesták–Berggren model produces the explicit rate equation (Eq. (15)):

$$\frac{d\alpha}{dt} = 1.46 \times 10^8 \exp\left(\frac{-58820}{RT}\right)\alpha^{0.460}(1-\alpha)^{1.44}\,\alpha \in [0, 1] \quad (15)$$

The experimental reaction rate (discrete dot) and model predications (full line) from Eq. (15) are compared in Fig. 7 directly from which a good agreement is observed. Therefore, Eq. (15) is adequate to model the nonisothermal reaction rate of DGEBA/TADH; the model-fitting kinetic study has achieved a satisfactory success.

3.5. E_α–α dependence

In fact, reactions of epoxy resins are extremely complicated processes involving various possible elementary reaction pathways, complex mass transfer processes, and a number of physico-chemical transitions [6]. Consequently, using a single reaction rate equation to accurately untangle these complexities often yields very vague results [46], because it is practically impossible to take

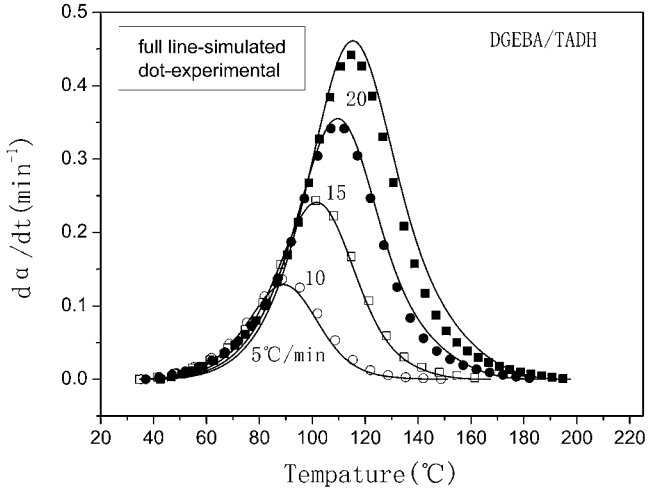

Fig. 7. Comparison of predicated rates from Šesták–Berggren model and experimental rates.

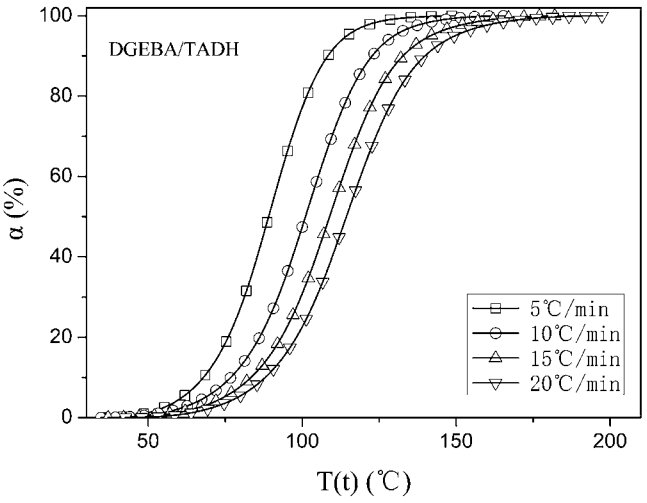

Fig. 8. Variation of α with T at heating rates of 5, 10, 15 and 20 °C/min.

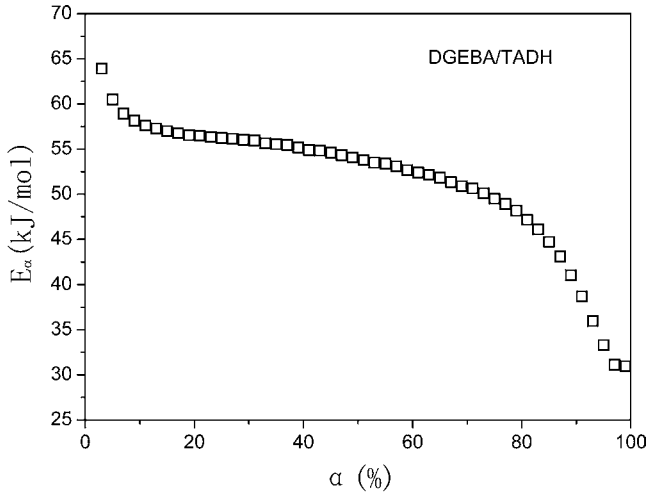

Fig. 9. Variation of effective activation energy E_α with conversion α.

all these complexities into account with a single rate equation. Similarly, the simple rate equation (Eq. (15)) is able to well describe the isothermal reaction rate of DGEBA/TADH on a macroscopic level, undoubtedly, which is a good help for practical predication of reaction rates, but it is still insufficient to give a relatively clear profile of the reaction mechanisms. Fortunately, the model-free isoconversional kinetic analysis can partially overcome this limitation, since it can provide more direct kinetic information, independent of any specific models. Specifically, the variation in effective activation energy E_α with conversion α can be identified using an advanced model-free isoconversional method (Vyazovkin method) with great precision. This E_α–α correlation usually corresponds to change of reaction mechanisms; it may reflect relative contributions of parallel reaction channels to overall reaction kinetics [100]. In this work, we have used the Vyazovkin method, for the first time, to analyze the mechanisms of the nonisothermal reaction of DGEBA/TADH.

Fig. 8 plots α as a function of $T(t)$ for the different heating rates. As seen, with increasing the heating rates, the conversional curves shift towards a higher and broader temperature region, which indicates the reaction rate is an increasing function of the temperature. Introduce the α–$T(t)$ data into Eqs. (9) and (10), and E_α for each α can be determined by minimizing Eq. (9) using a home-made program based upon the Matlab® (R2007b) Software interface, as presented in Fig. 9 where E_α is plotted as a function of α. Clearly, E_α changes greatly with α, which is a strong indicator that the nonisothermal reaction of DGEBA/TADH probably follows multi-step mechanisms [62], as specified below.

As seen in Fig. 9, E_α decreases from >65 to ~57 kJ/mol up to $\alpha \approx 15\%$, which quite resembles our previous finding for the nonisothermal reaction of DGEBA/MXBDP [6], associated with somewhat change of the reaction mechanisms. The following two reasons may account for this observation. First, the secondary –OH functionalities generated during the epoxy-amine addition can greatly catalyze the remaining epoxy-amine reaction via a trimolecular transition state, particularly an activated epoxy-amine-hydroxyl complex [88,101–103]. Second, the viscosity of the reaction mixture decreases dramatically with increasing the temperature at this stage, which promotes diffusion of the reactive species [78]. As a result, the respective energetic barriers for the reaction itself and the diffusion decrease simultaneously, thus further lowering overall E_α at the early reaction stage.

As α increases from 15 to 75%, E_α decreases slowly from ~57 to 50 kJ/mol. This observation may indicate that the reaction still controls the overall reaction kinetics, and the diffusion control seems less influential, even though the gelation of the reaction mixture occurs is this stage ($\alpha_{gel} = 0.378$) [104]. In other words, the reaction still progresses in the reaction-controlled regime even after the gelation. It is worth pointing out that the previous research has demonstrated that remarkable decrease of E_α for the nonisothermal reactions of DGEBA/MXBDP (aliphatic amine, $f = 8$) [6] and DGEBA/1,3-phenylenediamine (aromatic amine, $f = 4$) [79] took place close to α_{gel}. In this study, however, the decrease of E_α at α_{gel} is less distinctive, which implicates that amine hardeners influence greatly microscopic mechanisms of epoxy-amine reactions. To illustrate, their functionalities, molecular structure, chain flexibility, element composition, and nature of amine functionalities (aliphatic or aromatic) may affect the diffusion-complicated reaction kinetics to different degrees. More specifically, comparing the DGEBA/TADH and DGEBA/MXBDP [6] systems, we can infer that TADH with the more flexible hexamethylene spacer leads to the corresponding nonisothermal reaction is less influenced by the diffusion near the gelation than MXBDP bearing the more rigid benzene core.

Finally, as the reaction progresses in the deep-conversion range ($\alpha > 0.75$), E_α decreases abruptly from ~50 to 30 kJ/mol. This fact implies the rate-determining step of the reaction generally changing from the reaction control to the diffusion limitation, which fairly resembles the previous finding for DGEBA/1,3-phenylenediamine system [79]. The reason lies in that the mobility of the molecular chains carrying the reactive species becomes more and more limited due to the increased junction points and the gradually elevated glass temperature which greatly restrict configuration rearrangements and cooperative motions of the network chains, especially as the reaction system approaches its glassy state [103].

3.6. Thermal stability of cured epoxy

Thermal stability of the cured DGEBA/TADH and DGEBA/hexanediamine were evaluated with TGA in a comparative manner. Fig. 10 illustrates the weight percent as a function of temperature for DGEBA/TADH and DGEBA/hexanediamine at the heating rate of 10 °C/min under N_2. Clearly, no obvious weight loss appears up to 300 °C, after which a quick drop in weight occurs within 300–500 °C, and the initial thermal decomposition temperature of the former is slightly lower than that of the latter. This result suggests that like linear hexanediamine, TADH can impart the cured epoxy resin with sufficient good thermal stability. In addition, DGEBA/TADH exhibits the increased content of the residual char at 600 °C compared with DGEBA/hexaediamine,

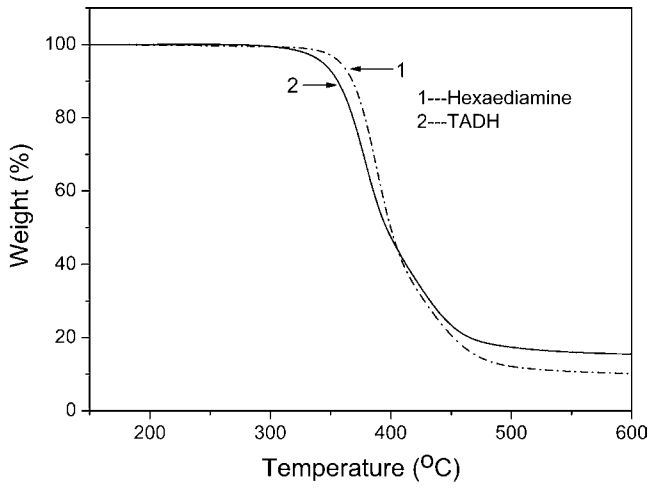

Fig. 10. TG thermograms of DGEBA/TADH and DGEBA/hexanediamine at heating rate of 10 °C/min in N_2.

which indicates TADH can moderately improve the flame retardance of the resulting epoxy materials, lowering the production of combustible gases [105]. A probable reason for this observation is that TADH enhances the crosslink density of the resulting epoxy network, which in turn increases chemical bonds needed be broken to generate volatile gases, further promoting the char formation during the thermal decomposition process in N_2.

3.7. Dynamic mechanical properties of epoxy network

Presented in Fig. 11 is the dynamic mechanical spectrum for storage modulus E' and loss factor Tan δ as a function temperature T from −100 °C to well above the glass temperature of the fully cured DGEBA/TADH network. In addition, some characteristic relaxation temperatures and storage modulus obtained from the DMA spectrum are listed in Table 4. Obviously, the network exhibits high stiffness from room temperature up to 80 °C (e. g., E'(20 °C) = 2617 MPa and E'(80 °C) = 1649 MPa), and E' and Tan δ show a strong temperature dependence. For instance, in a higher temperature range (>100 °C), E' drops rapidly with T; meanwhile, Tan δ increases dramatically going through its maximum. These phenomena are associated with the glass relaxation of the epoxy networks arising from cooperative motions of the chain segments of the network, and the glass temperature T_g is 136.7 °C corresponding to Tan δ_{max}. Moreover, the DGEBA/TADH network has the comparable T_g value with a number of epoxy networks with conventional linear aliphatic amine hardeners [27,30,31,106–108], and in particular this value is higher than literature value for the DGEBA/hexanediamine network (118–121 °C) [30,31], indicating its improved thermal-mechanical properties. Noticeably, a weak but broad secondary relaxation (β relaxation) emerges in the lower temperature region (about −100 to −10 °C), and its relaxation temperature T_β for Tan δ_{max} is −38.4 °C, which quite resembles that observed in other epoxy networks with linear amine hardeners. This relaxation can be assigned to the localized crankshaft movement of the hydroxyl ether segments (–$CH_2CH(OH)CH_2O$–) in the network generated during the epoxy-amine addition [32,109–111], which implies that nonlinear molecular architecture of TADH dose not alter the fundamental mechanisms of secondary relaxations of epoxy-amine networks.

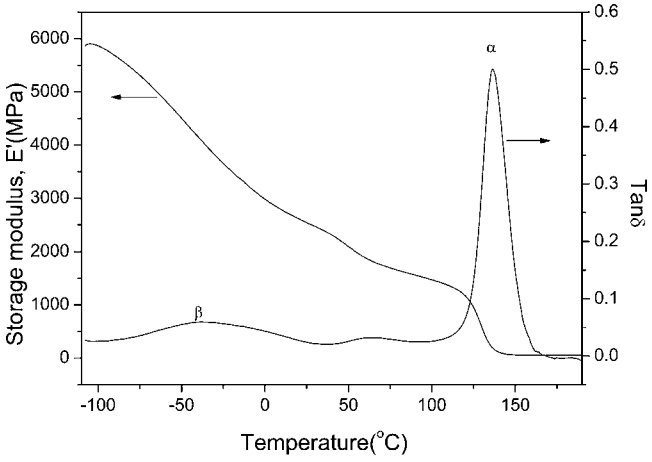

Fig. 11. Dynamic mechanical spectra for E' and Tan δ vs. temperatures T of DGEBA/TADH network at oscillation frequency of 1 Hz and heating rate of 3 °C/min.

Table 4
Characteristic relaxation temperatures and storage modulus of DGEBA/TADH network.

Formulation	DGEBA/TADH
α Relaxation (T_g)/°C	136.7
β Relaxation (T_β)/°C	−38.4
Modulus at −100 °C/MPa	5865
Modulus at 20 °C/MPa	2617
Modulus at 80 °C/MPa	1649
Rubber modulus (T_g + 30) /MPa	56

4. Conclusions

We have successfully prepared TADH and found it can effectively cure DGEBA. The overall nonisothermal reaction exotherm was in 117.8–121.2 kJ/mol epoxide, the apparent reaction activation energy was 58.82 kJ/mol, and the Šesták–Berggren model could well model the reaction rate. The correlation of the effective activation with conversion indicated in general the reaction control took the dominant role in the overall kinetics during the early stages of the reaction, and the viscosity and the autocatalysis were moderately influential, whereas in the deep-conversion region ($\alpha > 0.75$) the diffusion limitation became much predominant. Moreover, TADH could impart the cured epoxy resin with the sufficient good thermal stability with improved residual char content in N_2 compared with linear hexanediamine. Furthermore, the DGEBA/TADH network exhibited the good dynamic mechanical properties, and its glass temperature and secondary relaxation temperature were 136.7 and −38.4 °C, respectively. In summary, TADH may find a promising application in practical epoxy formulations, particularly in room temperature–cure epoxy coatings and adhesives.

Acknowledgements

The authors would like to acknowledge financial support of this work from the Major Research Project of Zhejiang Province (grant no. 2006C11192) sponsored by the Science and Technology Department of Zhejiang Province, China. The authors also wish to give special thanks to the reviewers for their comments of great value and the editors for their hard work.

References

[1] E.M. Petrie, Epoxy Adhesive Formulations, McGraw-Hill Publishing, 2006.
[2] C.A. May, Epoxy Resins Chemistry and Technology, 2nd ed., Marcel Dekker, Inc., 1988.
[3] H.Q. Pham, M.J. Marks, Encyclopedia of Polymer Science and Technology, Wiley & Sons Inc., 2004.
[4] S. Lu, W. Chun, J. Yu, X. Yang, J. Appl. Polym. Sci. 109 (2008) 2095–2102.

[5] H.S. Chu, J.C. Seferis, Polym. Compos. 5 (1984) 124–140.
[6] J. Wan, B.-G. Li, H. Fan, Z.-Y. Bu, C.-J. Xu, Thermochim. Acta (2010), doi:10.1016/j.tca.2010.1006.1021.
[7] L. Xu, J.H. Fu, J.R. Schlup, J. Am. Chem. Soc. 116 (1994) 2821–2826.
[8] M. Opaliki, J.M. Kenny, L. Nicolais, J. Appl. Polym. Sci. 61 (1996) 1025–1037.
[9] D. Roşu, F. Mustaţă, C.N. Caşcaval, Thermochim. Acta 370 (2001) 105–110.
[10] M. Frigione, E. Calò, J. Appl. Polym. Sci. 107 (2007) 1744–1758.
[11] B.K. Kandola, B. Biswas, D. Price, A.R. Horrocks, Polym. Degrad. Stabil. 95 (2009) 144–152.
[12] S.R. Patel, V.S. Patel, R.G. Patel, Thermochim. Acta 182 (1991) 319–327.
[13] S.-N. Lee, M.-T. Chiu, H.-S. Lin, Polym. Eng. Sci. 32 (1992) 1037–1046.
[14] L. Chiao, Macromolecules 23 (1990) 1286–1290.
[15] R.H. Patel, R.G. Patel, Thermochim. Acta 160 (1990) 323–328.
[16] R.H. Patel, R.G. Patel, Thermochim. Acta 173 (1990) 95–100.
[17] A. Padma, R.M.V.G.K. Rao, C. Subramaniam, G. Nagendrappa, J. Appl. Polym. Sci. 57 (1995) 401–411.
[18] R.D. Pate, R.G. Patel, V.S. Patel, J. Therm. Anal. Calorim. 43 (1988) 1283–1293.
[19] Y. Cheng, T. Xu, P. He, J. Appl. Polym. Sci. 103 (2007) 1430–1434.
[20] D.-M. Xu, K.-D. Zhang, X.-L. Zhu, J. Appl. Polym. Sci. 101 (2006) 3902–3906.
[21] Y. Cheng, D. Chen, R. Fu, P. He, Polym. Int. 54 (2005) 495–499.
[22] H. Cai, P. Li, G. Sui, Y. Yu, G. Li, X. Yang, S. Ryu, Thermochim. Acta 473 (2008) 101–105.
[23] P. Budrugeac, E. Segal, Polym. Degrad. Stabil. 93 (2008) 1073–1080.
[24] M.P. Luda, A.I. Balabanovich, M. Zanetti, D. Guaratto, Polym. Degrad. Stabil. 92 (2007) 1088–1100.
[25] E.M. Woo, J.C. Seferis, R.S. Schaffnit, Polym. Compos. 12 (1991) 273–280.
[26] M. Xie, Z. Zhang, Y. Gu, M. Li, Y. Su, Thermochim. Acta 487 (2009) 8–17.
[27] L. Barral, J. Cano, A. López, P. Nogueira, C. Ramírez, J. Therm. Anal. Calorim. 41 (1994) 1463–1467.
[28] S. Cukierman, J.-L. Halary, L. Monnerie, Polym. Eng. Sci. 31 (1991) 1476–1482.
[29] L. Heux, J.L. Halary, F. Lauprêtre, L. Monnerie, Polymer 38 (1997) 1767–1778.
[30] J.F. Gerard, J. Galy, J.P. Pascault, S. Cukierman, J.L. Halary, Polym. Eng. Sci. 31 (1991) 615–621.
[31] L. Heux, F. Lauprêtre, J.L. Halary, L. Monnerie, Polymer 39 (1998) 1269–1278.
[32] G.W. John, J. Appl. Polym. Sci. 23 (1979) 3433–3444.
[33] E. Urbaczewski-Espuche, J. Galy, J.-F. Gerard, J.-P. Pascault, H. Sautereau, Polym. Eng. Sci. 31 (1991) 1572–1580.
[34] M.J. Marks, N.E. Verghese, K.J. Hrovat, A. Laboy-Bollinger, J.C. Buck, J.A. Rabon Jr., C.L. O'connell, L. Allen, J. Polym. Sci. B: Polym. Chem. 46 (2008) 1632–1640.
[35] R.J. Morgan, F.-M. Kong, C.M. Walkup, Polymer 25 (1984) 375–386.
[36] E.M.M. de Brabander-van den Berg, E.W. Meijer, Angew. Chem. Int. Ed. Engl. 32 (1993) 1308–1311.
[37] C. Wörner, R. Mülhaupt, Angew. Chem. Int. Ed. Engl. 32 (1993) 1306–1308.
[38] J.M. Barton, Adv. Polym. Sci. 72 (1985) 111–154.
[39] G. Micco, M. Giamberini, E. Amendola, C. Carfagna, G. Astarita, Ind. Eng. Chem. Res. 36 (1997) 2976–2983.
[40] R. Fernándeza, B.F. d'Arlasa, P.A. Oyangurenb, I. Mondragon, Thermochim. Acta 493 (2009) 6–13.
[41] R.A. Fava, Polymer 9 (1968) 137–151.
[42] M.E. Brown, P.K. Gallagher, Handbook of Thermal Analysis and Calorimetry, vol. 5, Elsevier Science and Technology, 2008.
[43] J. Málek, Thermochim. Acta 200 (1992) 257–269.
[44] J. Málek, J.M. Criado, Thermochim. Acta 203 (1992) 25–30.
[45] S. Monserrat, J. Málek, Thermochim. Acta 228 (1993) 47–60.
[46] S. Vyazovkin, C.A. Wight, Thermochim. Acta 340–341 (1999) 53–68.
[47] J. Málek, J. Sesták, Thermochim. Acta 203 (1992) 31–42.
[48] G. Tripathi, D. Srivastava, J. Appl. Polym. Sci. 112 (2009) 3119–3126.
[49] D. Rosu, A. Mititelu, C.N. Cascaval, Polym. Test 23 (2004) 209–215.
[50] G. Xu, W. Shi, S. Shen, J. Polym. Sci. B: Polym. Chem. 42 (2004) 2649–2656.
[51] D. Rou, C.N. Cacaval, F. Musta, C. Ciobanu, Thermochim. Acta 383 (2002) 119–127.
[52] S. Montserrat, G. Andreu, P. Cortés, Y. Calventus, P. Colomer, J.M. Hutchinson, J. Málek, J. Appl. Polym. Sci. 61 (1996) 1663–1674.
[53] S. Montserrat, C. Flaqué, P. Pagès, J. Málek, J. Appl. Polym. Sci. 56 (1995) 1413–1421.
[54] S. Montserrat, C. Flaqué, M. Calafell, G. Andreu, J. Málek, Thermochim. Acta 269–270 (1995) 213–229.
[55] M.J. Yoo, S.H. Kim, S.D. Park, W.S. Lee, J.-W. Sun, J.-H. Choi, S. Nahm, Eur. Polym. J. 46 (2010) 1158–1162.
[56] J. Gao, D. Kong, S. Li, Polym. Compos. 31 (2010) 60–67.
[57] J. Gao, X. Zhang, L. Huo, H. Zhao, J. Therm. Anal. Calorim. 100 (2010) 225–232.
[58] L. Yao, J. Deng, B.-j. Qu, W.-f. Shi, Chem. Res. Chin. Univ. 22 (2006) 118–122.
[59] F. Wang, J. Xiao, J.-W. Wang, S.-Q. Li, J. Appl. Polym. Sci. 107 (2007) 223–227.
[60] J.H. Flynn, Thermochim. Acta 300 (1997) 83–92.
[61] G.I. Senum, R.T. Yang, J. Therm. Anal. Calorim. 11 (1977) 445–447.
[62] S. Vyazovkin, N. Sbirrazzuoli, Macromol. Rapid Commun. 20 (1999) 387–389.
[63] L.F. Henry, J. Polym. Sci. C 6 (1964) 183–195.
[64] S. Vyazovkin, N. Sbirrazzuoli, Macromol. Rapid Commun. 27 (2006) 1515–1532.
[65] S. Vyazovkin, D. Dollimore, J. Chem. Inf. Comput. Sci. 36 (1996) 42–45.
[66] C.D. Doyle, J. Appl. Polym. Sci. 6 (1962) 639–642.
[67] A.W. Coats, J.P. Redfern, Nature 201 (1964) 68–69.
[68] T. Ozawa, Bull. Chem. Soc. Jpn. 38 (1965) 1881–1886.
[69] J.H. Flynn, L.A. Wall, J. Res. Natl. Bur. Stand. A: Phys. Chem. 70A (1966) 487–523.
[70] S. Vyazovkin, J. Comput. Chem. 18 (1997) 393–402.
[71] S. Vyazovkin, J. Comput. Chem. 22 (2001) 178–183.
[72] J. Cai, S. Chen, J. Comput. Chem. 30 (2009) 1986–1991.
[73] S. Vyazovkin, A. Mititelu, N. Sbirrazzuoli, Macromol. Rapid Commun. 24 (2003) 1060–1065.
[74] Y. Zhang, S. Vyazovkin, J. Phys. Chem. B 111 (2007) 7098–7104.
[75] N. Sbirrazzuoli, S. Vyazovkin, Thermochim. Acta 388 (2002) 289–298.
[76] S. Vyazovkin, N. Sbirrazzuoli, Macromol. Chem. Phys. 200 (1999) 2294–2303.
[77] S. Vyazovkin, N. Sbirrazzuoli, Macromol. Rapid Commun. 21 (2000) 85–90.
[78] S. Vyazovkin, N. Sbirrazzuoli, Macromol. Chem. Phys. 201 (2000) 199–203.
[79] N. Sbirrazzuoli, S. Vyazovkin, A. Mititelu, C. Sladic, L. Vincent, Macromol. Chem. Phys. 204 (2003) 1815–1821.
[80] Y. Zhang, S. Vyazovkin, Macromol. Chem. Phys. 206 (2005) 1084–1089.
[81] Y. Zhang, S. Vyazovkin, Macromol. Chem. Phys. 206 (2005) 342–348.
[82] Y. Zhang, S. Vyazovkin, Macromol. Chem. Phys. 206 (2005) 1840–1846.
[83] Y. Zhang, S. Vyazovkin, Polymer 47 (2006) 6659–6663.
[84] Z.-Q. Cai, J. Sun, D. Wang, Q. Zhou, J. Polym. Sci. A: Polym. Chem. 45 (2007) 3922–3928.
[85] H. Ren, J. Sun, Q. Zhao, C. Zhiqi, Q. Ling, Q. Zhou, J. Appl. Polym. Sci. 112 (2009) 761–768.
[86] G. Li, Z. Huang, P. Li, C. Xin, X. Jia, B. Wang, Y. He, S. Ryu, X. Yang, Thermochim. Acta 497 (2010) 27–34.
[87] N. Sbirrazzuoli, A. Mititelu-Mija, L. Vincent, C. Alzina, Thermochim. Acta 447 (2006) 167–177.
[88] B.A. Rozenberg, Adv. Polym. Sci. 75 (1986) 113–165.
[89] J.-Y. Lee, M.-J. Shim, S.-W. Kim, Thermochim. Acta 371 (2001) 45–51.
[90] V.L. Zvetkov, R.K. Krastev, V.I. Samichkov, Thermochim. Acta 478 (2008) 17–27.
[91] R. Sanctuary, J. Baller, B. Zielinski, N. Becker, J.K. Kruger, M. Philipp, U. Muller, M. Ziehmer, J. Phys. Condens. Matter 21 (2009) 035118.
[92] V.L. Zvetkov, Polymer 42 (2001) 6687–6697.
[93] H.J. Flammersheim, Thermochim. Acta 296 (1997) 155–159.
[94] H.J. Flammersheim, Thermochim. Acta 310 (1998) 153–159.
[95] H.E. Kissinger, Anal. Chem. 29 (1957) 1702–1706.
[96] V.L. Zvetkov, R.K. Krastev, S. Paz-Abuin, Thermochim. Acta 505 (2010) 47–52.
[97] V.L. Zvetkov, Polymer 43 (2002) 1069–1080.
[98] F.-X. Perrin, T.M.H. Nguyen, J.-L. Vernet, Macromol. Chem. Phys. 208 (2007) 718–729.
[99] J. Šesták, G. Berggren, Thermochim. Acta 3 (1971) 1–12.
[100] G.-H. Hsiue, H.-F. Wei, S.-J. Shiao, W.-J. Kuo, Y.-A. Sha, Polym. Degrad. Stabil. 73 (2001) 309–318.
[101] V.L. Zvetkov, Thermochim. Acta 435 (2005) 71–84.
[102] I.T. Smith, Polymer 2 (1961) 95–108.
[103] S. Vyazovkin, N. Sbirrazzuoli, Macromolecules 29 (1996) 1867–1873.
[104] G. Odian, Principles of Polymerization, Fourth ed., John Wiley & Sons, Inc., 2004.
[105] Y.L. Liu, C.S. Wu, K.Y. Hsu, T.C. Chang, J. Polym. Sci. A: Polym. Chem. 40 (2002) 2329–2339.
[106] T. Kamon, H. Furukawa, Adv. Polym. Sci. 80 (1986) 173–202.
[107] F.G. Garcia, B.G. Soares, V.J.R.R. Pita, R. Sánchez, J. Rieumont, J. Appl. Polym. Sci. 106 (2007) 2047–2055.
[108] F.F.D. Nograro, P. Guerrero, M.A. Corcuera, I. Mondragon, J. Appl. Polym. Sci. 56 (1995) 177–192.
[109] O. Delatycki, J.C. Shaw, J.G. Williams, J. Polym. Sci. B: Polym. Chem. 7 (1969) 753–762.
[110] S.A. Paipetis, P.S. Theocaris, A. Marchese, Colloid Polym. Sci. 257 (1979) 478–485.
[111] M. Ochi, M. Okazaki, M. Shimbo, J. Polym. Sci. B: Polym. Phys. 20 (1982) 689–699.